DUNPHY, ANDREW M., M.S. Modulation of Macrophage Polarization by Carbon Nanodots. (2020)
Directed by Dr. Zhenquan Jia. 50 pp.

Atherosclerosis represents an ever-present global concern, as it is a leading cause of cardiovascular disease, and an immense public welfare issue. Macrophages play a key role in the onset of the disease state. Free oxygen radicals modify low-densitiy lipoprotieins (LDL) into ox-LDL. Upon injury to the endothelium of blood vessels by ox-LDL, circulating monocytes differentiate into pro-inflammatory (M1) or anti-inflammatory (M2) macrophages. In progressing lesions, M1 macrophages engulf excess ox-LDL. In the process, these macrophages become lipid-laden and lose mobility, finally proceeding to settle en-masse on the bed of arteries as plaque. Dysregulated plaque build-up in arteries results in a several fatal long-term health issues. Due to their crucial role as mediators in atherogenesis, as well as their involvement in several aspects of the immune response, macrophages are popular targets in vascular research and therapeutic treatment. Carbon nanodots (CNDs) represent a type of carbon-based nanomaterial, and have garnered attention in recent years for potential in biomedical applications. CNDs have various attractive qualities that have made them useful for several applications, including biosensing and drug delivery. A key feature of CNDs is their capability for free radical scavenging ability. However, no reports exist analyzing the interaction of CNDs and macrophages.

This investigation serves as a foremost attempt at characterizing the interplay between macrophages and CNDs. We have employed THP-1 monocyte-derived macrophages as our target cell line representing primary macrophages in the human

body. Our results showcase that CNDs are non-toxic at a variety of doses. THP-1 monocytes were differentiated into macrophages by treatment with 12-*O*-tetradecanoylphorbol-13-acetate (TPA), and co-treated with 0.1 mg/mL CNDs. This co-treatment significantly increased the expression of CD 206 and CD 68 (key receptors involved in phagocytosis), and reduced the expression of CCL2 (a monocyte chemoattractant and pro-inflammatory cytokine). The phagocytic activity of THP-1 monocyte-derived macrophages co-treated with 0.1 mg/mL CNDs also showed a significant increase. Furthermore, our project aimed at determining potential entrance and exit routes of CNDs into macrophages. We have demonstrated an inhibition in the uptake of CNDs in macrophages treated with nocodazole (microtubule disruptor), N-phenylanthranilic acid (chloride channel blocker), and mercury chloride (aquaporin channel inhibitor). Lastly, our data denotes a significant increase in the release of CNDs when macrophages were also treated with nocodazole. Collectively, this research provides evidence that CNDs cause functional changes in macrophages, and indicates a variety of potential entrance and exit routes.

MODULATION OF MACROPHAGE POLARIZATION BY CARBON NANODOTS

by

Andrew M. Dunphy

A Thesis Submitted to
the Faculty of The Graduate School at
The University of North Carolina at Greensboro
in Partial Fulfillment
of the Requirements for the Degree
Master of Science

Greensboro
2020

Approved by

_____
Committee Chair

APPROVAL PAGE

This thesis written by Andrew M. Dunphy has been approved by the following committee of the Faculty of The Graduate School at the University of North Carolina at Greensboro

Committee Chair_____

Committee Members_____

_____

_____
Date of Acceptance by Committee

_____
Date of Final Oral Examination

TABLE OF CONTENTS

Page

LIST OF TABLES

Page

LIST OF FIGURES

Page

CHAPTER I

INTRODUCTION

The Toll of Cardiovascular Disease

Cardiovascular disease (CVD) has more clinical implications than any other condition worldwide. Globally, CVD accounts for a third of all deaths. In the United States, over 600,000 humans die of CVD per year, representing a quarter of all American deaths. For these reasons, devoting resources and research into ameliorating the mortality caused by CVD is of principal priority. CVD can be expressed in several types such as ischemic heart disease, cerebrovascular disease, rheumatic heart disease, or endocarditis [1]. Several types of cardiovascular disease are characterized by the presence of atherosclerosis, which is the build-up of plaque in artery walls. This condition leads to a decrease in blood flow to tissues. With the ever-increasing mortality rate due to CVD, it is crucial to develop new methods of treatment. The biggest challenge still is understanding the ramifications of the development of atherosclerosis.

Progression and Biomarkers of Atherosclerosis

The inception of atherosclerosis is first characterized by the intrusion of low-density lipoproteins (LDL) into the arterial intima of a blood vessel. At this site, LDL undergoes oxidation by reactive oxygen species (ROS), and as a result, becomes a much more reactive particle. This can cause inflammation of the endothelium [2]. The injured ECs release adhesion molecules which recruit leukocytes (such as monocytes). These, in

turn, secrete several inflammatory cytokines and chemokines [3]. The monocytes differentiate into macrophages, which ingest ox-LDL, and turn into foam cells that settle on the bed of the artery as plaque. The resulting foam cells, as well as macrophages, release metalloproteinases (MMPs) that are in charge of degrading the fibrous cap of the plaque [3]. As pieces of the plaque rupture, a thrombus can be formed, which may block blood vessels it navigates. Reduced blood flow to tissues ensues, which can have dangerous clinical repercussions such as myocardial infarction.

There are several biomarkers that help monitor states of atherosclerosis, but it is essential to realize how useful each one can be. C-reactive protein (CRP) is an acute-phase protein produced by the liver during inflammation events, and can be detected at sites of inflammation. That being said, CRP has poor specificity as a biomarker, given that it can be influenced by a variety of factors including smoking, hypertension, and other cardiovascular risks [3]. High-density lipoproteins (HDL) have been shown to inversely correlate with the incidence of cardiovascular events. HDLs exhibit protective blood vessel properties including antioxidant, anti-inflammatory, and cholesterol efflux capability, making them into a useful biomarker for atherosclerosis.

However, their use as a biomarker is better left for primary prevention, as the inverse correlation with CVD events is decreased in patients with more severe states such as chronic coronary heart disease [4]. Other useful biomarkers are cytokines and chemokines such as interleukin (IL) 6, IL-8, and tumor necrosis factor-alpha (TNF-α). Elevated levels of these molecules have been correlated with patients exhibiting ischemic cardiac disease and other cardiovascular dysfunctions. It should be noted, however, that

none of these molecules are solely specific to atherosclerosis [4]. The presence of adhesion molecules including monocyte chemoattractant protein-1 (MCP-1), vascular cell adhesion molecule-1 (VCAM-1), and intercellular adhesion molecule-1 (ICAM-1), as produced by inflamed ECs, can also indicate formation of plaque. Expression of these adhesion molecules is mediated by the nuclear factor kappa-light chain enhancer of activated B cells (NF-κB) signal transduction pathway, which is activated in the case of atherosclerosis by ox-LDL[5].

The Heterogeneity of Macrophages in Atherosclerosis

As the main developers of plaque, macrophages are largely responsible for the adverse effects of the condition. The bulk of the macrophages involved in the immune response to atherosclerosis are monocyte-derived, and can be classified traditionally as M1 (pro-inflammatory) or M2 (anti-inflammatory). As discussed previously, ECs release cytokines, chemokines, and adhesion molecules that recruit monocytes to the site of injury. A large part of these signals serve to differentiate monocytes into pro-inflammatory macrophages. M1 macrophages have several roles in the progression of atherosclerosis.

Uptake of modified lipoproteins in M1 macrophages occurs via scavenger receptors. Ox-LDL particles are transported to lysosomes, where they are degraded into free fatty acids and cholesterol. Free cholesterol can be trafficked into the endoplasmic reticulum (ER) to be re-esterified by enzymes [6]. These macrophages employ a number of transporters and mechanisms to remove re-esterified cholesterol, where it is then collected by HDL and apolipoprotein A-I [7]. As part of an early phase of atherosclerosis,

the result is beneficial. Removal of ox-LDL reduces the inflammation of the endothelium. However, excess accumulation of free cholesterol in macrophage ER membranes prevents their re-esterification, leading to increased storage. It is this imbalance of cholesterol influx/efflux that leads to macrophage conversion to foam cells. Subsequent ER stress can lead to cellular apoptosis. Ultimately, an excess of dying foam cells leads to their impaired clearance, partly due to impaired migratory ability, which contributes to a necrotic core forming within plaque [6].

Macrophages of the M1 classification can also release ROS. Dysregulation of ROS release can oxidize more lipoproteins, thereby exacerbating the inflammatory response. They also release pro-inflammatory cytokines such as IL-6, IL-1β, TNF-α, and granulocyte-macrophage stimulating factor (GM-CSF) so as to extend the pro-inflammatory response to other immune cells [8, 9]. GM-CSF was found to be heavily up-regulated in vessels suffering from atherosclerosis [10]. This up-regulation is a contributing factor to the predominance of M1 macrophages in vessels affected by plaque. M1 macrophages will also produce nitrous oxide (NO), synthesized by inducible nitrous oxide synthase (iNOS) when activated by pro-inflammatory signals [9].

In contrast, M2 macrophages are involved in the repair and remodeling of tissue [8, 9]. Induction of M2 macrophages occurs by Th2 cytokines such as IL-4 and IL-13 [11]. They secrete anti-inflammatory cytokines, including IL-10, which is involved in the reduction of reactive nitrogen species [12]. Induction by IL-4 leads to an up-regulation of resistin-like molecule alpha (FIZZ1), which promotes the synthesis of collagen to be used in tissue repair [11]. M2 macrophages also utilize arginine, induced by functional marker

Arginase-1, as a substrate of NO synthase, resulting in a decrease in nitrous oxide production [11]. M2 macrophages have also been implicated in regressing plaques, as high levels of MER proto-oncogene tyrosine kinase (MERTK) expression promotes efferocytosis of foam cells and dying macrophages [12].

Polarized macrophages also exhibit several biomarkers, ranging from functional, surface, and cytokine/chemokine receptors. M1 macrophages are well characterized by cluster of differentiation (CD)64 receptor and CD80 antigen[13]. Heterodimeric receptors interferon-gamma receptor (IFNGR)-1 and IFNGR-2 bind IFN-gamma and initiate signal cascades that lead to an M1 phenotype. CD 36 is a crucial scavenger receptor in M1 macrophages, responsible for absorbing ox-LDL [14]. M2 macrophages exhibit surface receptor CD 206, which functions to recognize carbohydrates in bacteria and yeast [15]. Other M2 surface receptors include CD11, CD23, CD163, and scavenger receptor A [8, 13, 15]. Several chemokine and cytokine receptors are also present in M2 macrophages that serve to suppress the immune response. These include c-c chemokine receptor type (CCR)3, CCR4, IL1R, and IL10RI and RII [15]. Arginase-1 provides ornithine for cellular repair and proliferation [15]. It should be noted that some markers are exhibited in both types of macrophages. The up-regulation of these markers depends on the stimuli [13].

Modern CVD Treatments

Currently there are a variety of treatment options for CVD, ranging from pharmacotherapy to surgical procedures. Although the list is extensive, progress remains underwhelming as several treatments are not without side effects and risks. Widely

recommended are statins, which serve as a form of lipid-lowering therapy. Statins competitively inhibit HMG CoA reductase, an essential enzyme in the synthesis of cholesterol by the human body [16]. As a result, LDL receptors in liver cells are upregulated, which helps clear cholesterol levels in blood [16]. However, the prevailing adverse effects of statin use are skeletal-muscle associated symptoms (SAMS), which include muscle pain, weakness, and fatigue. These symptoms may be due to mitochondrial dysfunction and impairment of the Akt pathway [17]. The use of human monoclonal antibodies is either too recent (and therefore not explored enough) or implicate side effects of their own. Canakinumab has been proven very effective at neutralizing IL-1β, but its clinical significance has only been confirmed in specific cases such as Muckle-Wells syndrome and neonatal-onset multisystem inflammatory disease [18]. Tocilizumab has been proposed as an IL-6 receptor antagonist to aide in patients suffering from rheumatoid arthritis, but results have shown that an increase in LDL is possible, which can only adversely impact CVD events [18].

Surgical procedures in patients suffering from various forms of CVD aim to revascularize blood vessels. Percutaneous coronary intervention may involve placing a stent within an artery to counter the narrowing produced by lesions. In carotid artery stenting, there is a risk for procedural stroke and re-narrowing of the blood vessel (restenosis) [19]. In patients with chronic limb-threatening ischemia (CLTI), bypass surgery is an option, although there is a risk of amputation upon failure of revascularization years post-surgery. As a whole, the prevailing risks of modern CVD treatments leave a demand for newer options with fewer side effects.

Carbon Nanodots: Potential Applications in Medicine

In recent years, interest in the development of nanoparticles for biological application has risen. A key area of intrigue revolves around the interaction of nanoparticles with some aspects of the immune response, resulting in their induction or repression [20]. Their use also extends to imaging macrophages and disease states such as atherosclerotic lesions [21, 22]. Nanomaterials are engineered from various sources such as silicates and metal oxides. They also possess ideal properties including reactivity, small sizing accompanied by membrane permeability, and increased solubility [20]. And yet, those same properties can give rise to toxicity. For instance, exposure of zinc oxide nanoparticles to rat lungs leads to pulmonary fibrosis, eosinophilia, and cell hyperplasia [23]. Much of the toxicity of nanoparticles can stem from the method of synthesis; heavy metal toxicity is always a concern. For this reason, research has recently been geared towards the creation of carbon-based nanoparticles. Carbon nanotubes, for instance, exhibit enhanced mechanical strength, electrical conductivity, and physicochemical stability [24]. These ideal properties, however, also allow them to be bio-resistant and hazardous. In animal studies, carbon nanotubes have demonstrated an ability to induce pulmonary fibrosis and toxicity [20, 24]. Carbon quantum dots (CQDs) demonstrate enhanced photostability and fluorescence, metabolic degradation resistance, and spectral features both narrow and tunable. Nonetheless, they are composed of toxic heavy metals, which severely limits their use [25].

Carbon nanodots (CNDs) are particles of particular interest for a variety of reasons. These particles tend to be smaller than 10 nm in size, have an sp2 hybridization,

and are quasi-spherical [26]. An essential characteristic of these nanodots is their high hydrophilicity, which is made apparent by the presence of several functional groups in their surface such as ether, carbonyl, hydroxyl, etc. This hydrophilicity allows for a very biocompatible particle, ready to interact with various organic or inorganic species [26]. CNDs also have photoluminescent properties. This, combined with their hydrophilicity, makes CNDs useful in sensing other particles. Their luminescent characteristics are defined by individual size, shape, functional groups, and other factors. Upon excitation by UV to visible light, CND emission wavelengths range from UV to near-infrared [26].

There are several methods to synthesize CNDs, including using all manner of organic molecules such as grass, coffee, and glucose molecules. Mainly, synthesis methods are categorized into either top-down approaches, or bottom-up approaches [26]. Top-down methods involve the breakdown of large, macroscopic carbon structures and are usually done under harsh conditions [26, 27]. Arc-discharge and laser ablation are popular top-down approaches [28]. Bottom-up applies external energy from a variety of sources (thermal, microwave, ultrasound irradiation, etc.) while using small organic molecules [27]. Using candle soot as a starting material, CNDs were synthesized by reflux with nitric acid [29]. Which specific methods are more reliable is the subject of debate, as each retains its own advantages and disadvantages.

CNDs have been synthesized with scavenging properties. This scavenging ability is heavily influenced by the method of synthesis, and as such, surface functional groups can be tailored to fit specific needs. In particular, CNDs with carboxylic surface groups have high affinity to mercury ions. This conjugation results in an absorbance band

detected at 302 nm, which only enhanced as the concentration of mercury ions increased [30]. CNDs prepared from citric acid tended to be more selective of Cu^{2+} ions. Preparation of CNDs with graphite rods revealed more selectivity towards Fe^{3+} ions, due to the formation of cupric amine and phenol hydroxyl complexes on their surfaces [26]. CNDs also proved themselves capable *ex vivo* scavengers of free radicals, one of which is 2,2-diphenyl-1-picrylhydrazyl radicals (DPPH•) [31]. In this assay, the successful conversion of DPPH• into a stable DPPH-H complex is due to antioxidant activity. This leads to a change in color from violet to light yellow, which can be quantified by ultraviolet-visible spectroscopy. Zhang et al. demonstrated a dose-dependent increase in DPPH• scavenging using N,S-codoped CNDs [31]. These nanoparticles were synthesized using citric acid, α-lipoic acid, and urea precursors through a hydrothermal method [32]. *In vitro*, CNDs have also demonstrated radical scavenging ability. By way of Di-Chloro Di-Hydrofuran Fluorescein Di-Acetate (DCFH-DA) assay and NBT (Nitro Blue Tetrazolium) reduction assay, Das et al. showcased CND (synthesized by microwave irradiation of date molasses) scavenging ability of hydroxyl and superoxide free radicals [33]. Altogether, these results denote the antioxidant propensity of CNDs and evidence their potential for biological utilization.

Atherosclerosis is a long-standing inflammatory disease, characterized by the narrowing of arteries due to a build-up of plaque. Overproduction of ROS and its subsequent oxidative stress play a key role in its initiation. Macrophages play an essential role as intermediators of the disease state by differentiating into a pro-inflammatory state, secreting cytokines and eventually becoming foam cells. As the concrete source for

plaque build-up, macrophages signify an area of interest. CNDs are a prospective choice for biomedical implementation, having shown usefulness in ROS scavenging, biosensing, and drug delivery. However, the antioxidant properties of CNDs on the polarization of macrophages has not been thoroughly researched. Currently, no account exists that indicates whether or not CNDs have any ability to affect the M1/M2 polarization of macrophages. In this study, we examined the effects of CNDs on the expression of M1/M2 biomarkers and phagocytic activity of macrophages, as well as potential entrance and exit routes.

CHAPTER II

MATERIALS AND METHODS

Cell Culture

THP-1 (ATCC® TIB-202™) cells were cultured in Roswell Park Memorial Institute 1640 Medium (RPMI 1640) fortified with 10% Fetal Bovine Serum (FBS) and 1% Penicillin-Streptomycin. This cell line was grown in Cellstar® Filter Cap 75cm^2 cell-culture treated, filter screw cap flasks in humidified incubators programmed to 37 °C and 5% CO_2. Corresponding media was renewed every 2 days and cells were split into a new passage upon 85%-90% confluence.

CND Synthesis

Using 0.96 g of citric acid, 1 mL of ethylenediamine, and 1 mL deionized water, Route 1 CNDs were synthesized by JSNN associates and collaborators in the Wei lab. Once mixed in glass vials, the solution was heated in a microwave reactor of 300 W for 18 minutes. The temperature was controlled below 150 °C as to produce a brownish solid, which in turn was dissolved in 5 mL DI water and dialyzed by a dialysis membrane with 1000 Da MWCO for a 24 hour period.

CND Characterization

UV-Vis spectroscopy of CNDs was performed by Cary® Eclipse TM Fluorescence Spectrophotometer. Upon dilution to 2 mg/mL in DI-H_2O, CNDs were

measured for fluorescence in a quartz cuvette to determine excitation and emission wavelengths.

Monocyte Differentiation into Macrophages

THP-1 cells were cultured in cell plates containing RPMI 1640 Medium or Sigma-Aldrich/Millipore Sigma® Hank's Balanced Salt Solution (HBSS) with calcium, magnesium, and glucose. Monocyte differentiation into macrophages was induced with 3 ng/µL of 12-O-tetra-decanoylphorbol-13-acetate (TPA) in an incubation period of 72 hr period. Cells were lifted by cell scraper and the supernatant placed in 50 mL Falcon tubes. Cell plates were rinsed with 2 mL PBS and also added to the supernatant. Cells were then pelleted by centrifuge.

CND Treatment

THP-1 monocytes were cultured in cell plates and co-treated with 0.1 mg/mL CNDs and 3 ng/µL TPA for 72 hours in RPMI media. Incubation occurred in 37°C/5% CO_2 incubators. Surrounding media was decanted and replaced with new media, followed by another incubation period of 72 hours. Cells were lifted by cell scraper and the supernatant placed in 50 mL Falcon tubes. Cell plates were rinsed with 2 mL PBS and also added to the supernatant. Cells were then pelleted by centrifuge.

Cell Count (Trypan Blue)

Before and after differentiation and CND treatments, cells were counted. Monocytes and macrophages were centrifuged at 300 g for 5 minutes at 4 °C and resuspended in either PBS or respective media. After resuspension, cells were counted

using a hemocytometer. Trypan blue was used to count viable, unstained cells, and the resulting concentration were also calculated.

RNA Extraction

THP-1 cells were cultured in appropriate media in Corning® cell culture treated plates. Upon treatment and incubation, adhered cells were lifted sing a cell scraper. The media was extracted into 50 mL tubes. The cell plates were rinsed twice with 1X PBS to ensure no treatment media remained and also to extract any remaining cells. Cells were then centrifuged at 300 g for 5 minutes at 4 °C. The supernatant media was decanted, and the resulting cell pellets treated with 1 mL of ambion TRIzol®. The resulting solution was pipetted into 1 mL Eppendorf tubes. 200 µL of Chloroform were added, followed by agitation, and then the solution was centrifuged at 12,000 rcf for 15 minutes. The top aqueous phase was transferred to another set of 1 mL Eppendorf tubes, and then combined with 500 µL isopropanol and agitated before centrifuging again at 12,000 rcf for 10 minutes. The resulting pellet (RNA) was washed with 1 mL 75% ethanol and centrifuged at 7,400 rcf for 5 minutes twice. The pellet was then resuspended in 10-15 µL of DEPC H_2O.

cDNA Synthesis

After RNA extraction, the resulting RNA was quantified by way of a Thermo Scientific™ Nanodrop 2000. Then, RNA was diluted to a concentration of 500 ng/µL. 2 µL of diluted RNA were mixed with 5 µL of 5X Buffer, 1.25 µL of ddNTP, 1.25 µL of Random Primer, 14.875 µL of DEPC H_2O, and 0.625 µL of MMLV-Reverse

Transcriptase. Using Applied Biosystems™ Veriti™ 96-Well Thermal Cycler, the 25 µL solution was converted to cDNA.

Quantitative Real Time Polymerase Chain Reaction

Once cDNA was synthesized using the methods above, the resulting cDNA was probed for a selection of M1/M2 biomarkers as mentioned previously, using H_GAPDH as a housekeeping gene. This was performed by mixing 1 µL of cDNA with 10 µL of Power SYBR® Green PCR Master Mix, 2 µL of 5 µM Forward Primer, 2 µL of 5 µM Reverse Primer, 2 µL of 1:10 diluted cDNA and 5 µL of DEPC H_2O. The Applied Biosystems™ StepOnePlus™ Real-Time PCR system was employed and ran for 40 cycles. Each individual cycle constituted a 95 °C phase for 15 seconds, a 58 °C phase for 60 seconds, and a 60 °C phase for 15 seconds. Comparative Threshold values were evaluated in order to quantify gene expression.

Vybrant™ Phagocytosis Assay Kit (V-6694)

4 x 10_6 THP-1 cells were grown in cell culture plates in corresponding media. Differentiation into macrophages was induced by administering 3 ng/µL TPA with an incubation period of 72 hours (with or without co-treatement with a CND concentration of 0.1 mg/mL) at 37 °C, 5% CO2. After harvesting and pelleting cells, concentration was re-suspended in HBSS to 2 x 10_6 cells/mL. 1 mL of control cells were treated with 1,000 ng/mL TPA in order to activate cells to serve as a positive control. Next, 100 µL of cell suspension was added to 5 wells per sample, plus 50 µL of HBSS (negative control wells contained 200 µL of HBSS). Cells were left to incubate for 18 hours in 35°C/5% CO_2 incubators. This incubation period allows macrophages to settle. HBSS was then

removed, and 200 µL of fluorescently-labeled *E.coli* suspension was administered for 2 hours. Upon removal of suspension, cells were treated for 60 seconds with 100 µL of Trypan Blue suspension. Immediate removal of suspension followed. The phagocytic activities of cells were quantified using a BioTek™ Synergy 2.0 plater reader.

ViaCount Flow Cytometry

Cells were cultured with the necessary incubation times and treatments. Next, cells were harvested by cell scraping and placed into tubes. The cell concentration was adjusted to 5 x 10_6/mL. 80 µL of cells were treated with 20 µL of ViaCount Reagent for 10 minutes at room temperature, upon which 500 µL of cold PBS was added. The samples were analyzed for viability using a Guava® easyCyte™ Flow Cytometer (Single Samples System).

CND Uptake + Inhibitors Protocol

THP-1 human monocyte-derived macrophages were grown to 85-90% confluence with corresponding media in clear cell plates and pre-treated with or without the following inhibitors for 30 minutes: Cytochalasin A or D (5 µg/mL), chlorpromazine (10 µg/mL), genistein (200 µM), nocodazole (20 µM), phenylglyoxal (100 ug/mL), amiloride hydrochloride (50 uM), n-phenylanthranilic acid (0.1mM), niflumic acid (10 mM), ebselen (15 uM), amiodarone hydrochloride(10 uM), chlorpromazine HCl (0.1 mg/mL), mercury chloride (0.075 mM), and copper sulfate (100 uM). Cells were then treated with a concentration of 0.1mg/mL CNDs for 24 hours. Cells were harvested and resuspended in PBS. Fluorescence was read at 360/460 top 400 nm in a well plate reader (Synergy 2.0).

CND Release + Inhibitors Protocol

THP-1 human monocyte-derived macrophages were grown to 85-90% confluence with corresponding media in clear cell plates and treated with a concentration of 0.1 mg/mL CNDs for 24 hours. After treatment, cells were washed with PBS three times, and resuspended in HBSS. Next, cells were treated with the same inhibitor concentrations as mentioned previously for 30 minutes. Cells were then centrifuged, and the supernatant removed and placed in a 96-well plate. CND released in HBSS was quantified by measuring the fluorescence of the supernatant in a plate reader using settings described previously.

Table 1. Primer Sequences for qrt-PCR Reactions

Target	**Forward Primer**	**Reverse Primer**
GAPDH	5'-AGA ACG GGA AGC TTG TCA TC-3'	5'-GGA GGC ATT GCT GAT GAT CT-3'
IL-8	5'-CTC TGT GTG AAG GTG CAG TT –3'	5' –AAA CTT CTC CAC AAC CCT CTG -3'
CCL-2	5'-GCT CAG CCA GAT GCA ATC AA-3'	5-GGT TGT GGA GTG AGT GGT CAA G-3'
CD68	5′-TCAGCTTTGGATTCATGCAG-3′	5′-AGGTGGACAGCTGGTGAAAG-3′
IL-10	5′-CTAACCTCATTCCCCAACCA-3′	5′-GTAGAGACGGGGTTTCACCA-3′
TNF-α	5′-CTATCTGGGAGGGGTCTTCC-3′	5′-GGTTGAGGGTGTCTGAAGGA-3′

CHAPTER III

RESULTS

Characterization of CNDs

CNDs to be used were characterized using a Cary fluorescence spectrophotometer. Excitation and emission wavelengths were determined by diluting CNDs to 0.06 mg/mL in DI-H_2O and measuring of fluorescence in a quartz cuvette. This concentration was specifically chosen because it generated a prominent peak, but with a gradual slope, while moderating the intensity of excitation and emission. The fluorescent spectrophotometer indicated a maximum excitation wavelength of 364 nm and a maximum emission wavelength of 458.9 nm (Fig. 2)

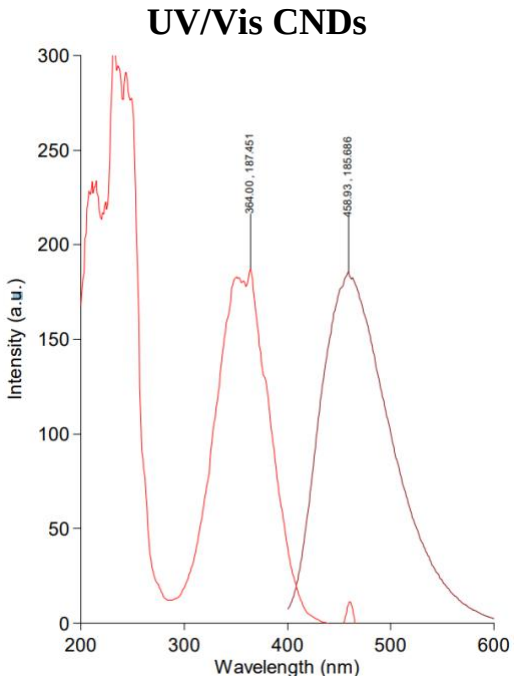

Figure 1. CND Excitation and Emission Spectra.
Cary Eclipse Fluorescence Spectrophotometer was utilized to measure intensity in of CNDs in a.u. Excitation peak is at 364 nm and an emission peak at 458.93 nm

Differentiation of THP-1 Monocytes

THP-1 monocytes were treated with 0, 1, 3, and 10 ng/mL TPA for 72 hours in RPMI media so as to stimulate the cells into differentiation. The media was then replaced and cells were allowed to incubate for an additional 72 hours. By way of qrt-PCR, expression of CD 206 (a macrophage differentiation marker) was assessed. As demonstrated by Figure 1, an increase in the expression of CD 206 ($P<0.05$) was observed in these TPA treated cells.

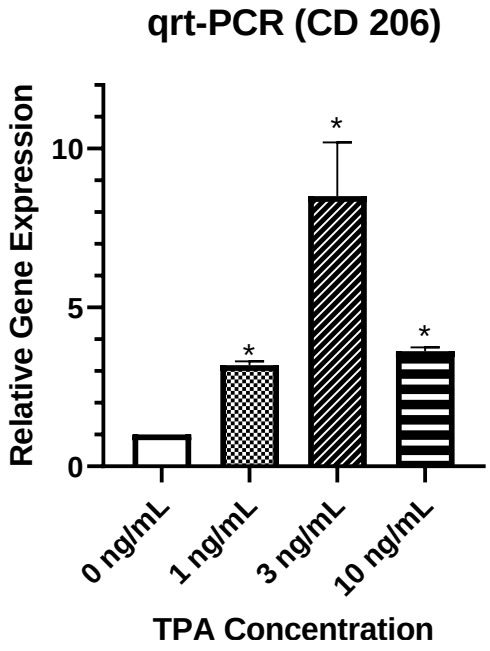

Figure 2. Increase in CD206 Expression in THP-1 Human Monocyte-derived Macrophages. THP-1 cells ($3.3x10_6$) were treated with 0, 1, 3, and 10 ng/mL of 12-O-tetradecanoylphorbol 13-acetate (TPA) in RPMI media for 72 hours, upon which media was refreshed. Cells were then left to incubate and mature for another 72 hours. RNA was isolated, converted to cDNA, and probed for CD206 using SYBR green qRT-PCR reagents via Biosystems™ StepOnePlus™ Software v2.3. GAPDH was the housekeeping gene. All data represent mean ± SEM. (n = 6, *, $P < 0.05$ vs. control).

Cell Viability Determined by Trypan Blue Cell Counts and ViaCount Flow Cytometry

In order to analyze the effect of CNDs on the viability of THP-1 monocyte-derived macrophages, I performed cell counts in a hemocytometer using Trypan Blue and performed ViaCount Flow Cytometry. The general concept behind the cell counts is that Trypan Blue can enter cells with a compromised membrane [34]. ViaCount reagent demonstrates effects on cell viability by using two DNA-binding dyes. One stains DNA in all cells, the other specifically binds to DNA in dead cells. THP-1 cells were treated with CND concentrations ranging from 0.01 to 0.6 mg/mL for 72 hours. After refreshing media, and an additional incubation period of 72 hours, cells were analyzed with both methods. The Trypan Blue cell counts demonstrate a significant decrease ($P<0.05$) in cell viability only at a concentration of 0.6 mg/mL (Fig. 3). Flow cytometric analysis demonstrates a significant reduction ($P<0.05$) in cell viability at 0.6 mg/mL CNDs (Fig 4a), and also that the percentage of live cells in the upper left quadrant only differ significantly ($P<0.05$) between untreated cells and cells treated with the same CND concentration (Fig. 4b).

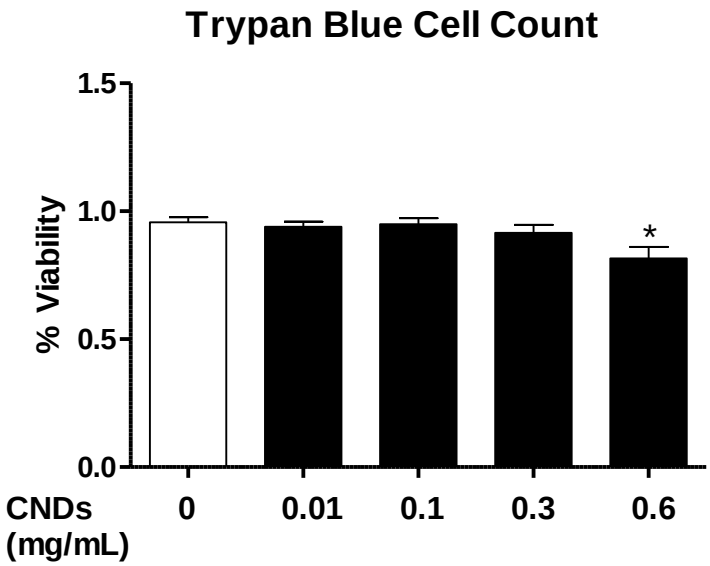

Figure 3. Effect of CNDs on Cell Viability (Trypan Blue). THP-1 cells were treated with 3 ng/mL TPA in the presence or absence of 0.01, 0.1, 0.3, or 0.6 mg/mL CNDs in RPMI media for 72 hours, upon which media was refreshed. Cells were then left to incubate for another 72 hours. Cells were harvested and a cell count performed using a hemocytometer and Trypan Blue. All data represent mean ± SEM. (n = 3, *, $P < 0.05$ vs. control).

A

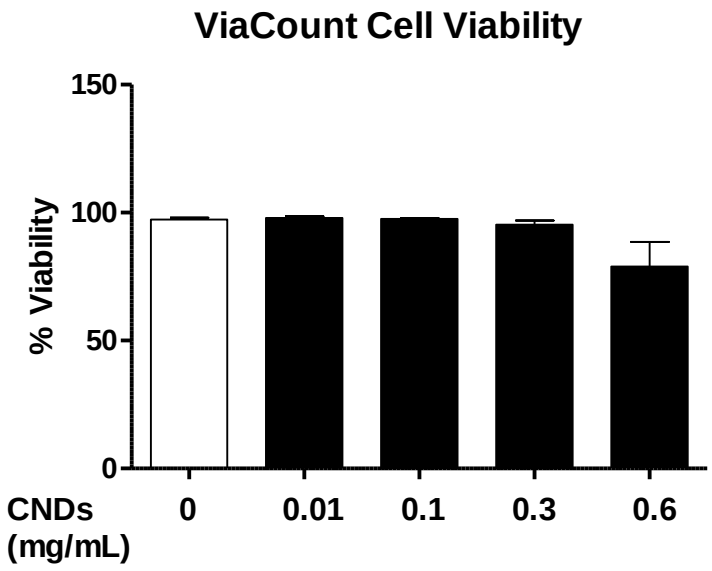

B

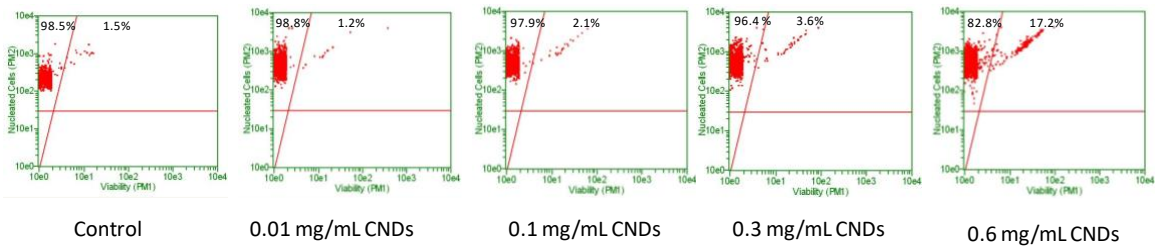

Figure 4. Effect of CNDs on Cell Viability (ViaCount). THP-1 cells were treated with 3 ng/mL TPA in the presence or absence of 0.01, 0.1, 0.3, or 0.6 mg/mL CNDs in RPMI media for 72 hours, upon which media was refreshed. Cells were then left to incubate for another 72 hours. Cells were then harvested and treated with ViaCount reagent. A viability analysis was then performed using a Guava® easyCyte™ Flow Cytometer (Single Sample System). All data represent mean ± SEM. (n = 3).

Expression of M1/M2 Biomarkers in Macrophages as Affected by CNDs

M1 (pro-inflammatory) macrophages play a crucial intermediary role in the atherosclerosis disease state. The effect of CNDs on the expression of M1 or M2 biomarkers was analyzed by PCR. THP-1 monocytes were co-treated with 3 ng/mL TPA and 0.1 mg/mL CNDs for 72 hours. These cells then had their media refreshed, followed by an additional incubation period of 72 hours. Cells were then harvested, RNA isolated, cDNA synthesized, and analyzed for expression of genes by qrt-PCR.

As previously mentioned, CD206 is a recognized M2 biomarker. IL-10 cytokine, which suppresses the immune response, was also analyzed as an M2 biomarker [15]. A selection of M1 biomarkers was included in the analysis. IL-8 and TNF-α are all well-established pro-inflammatory cytokines, also regarded as M1 biomarkers. CCL2 serves as a macrophage chemoattractant [9, 35]. CD68 is a surface receptor classified as an M1 biomarker. Our results indicate a significant increase ($P<0.05$) in CD 206, CD 68, and CCL2 expression in cells treated with 0.1 mg/mL CNDs. No significant effect was observed in the expression of TNF-alpha, IL-8, and IL-10 (Fig. 5).

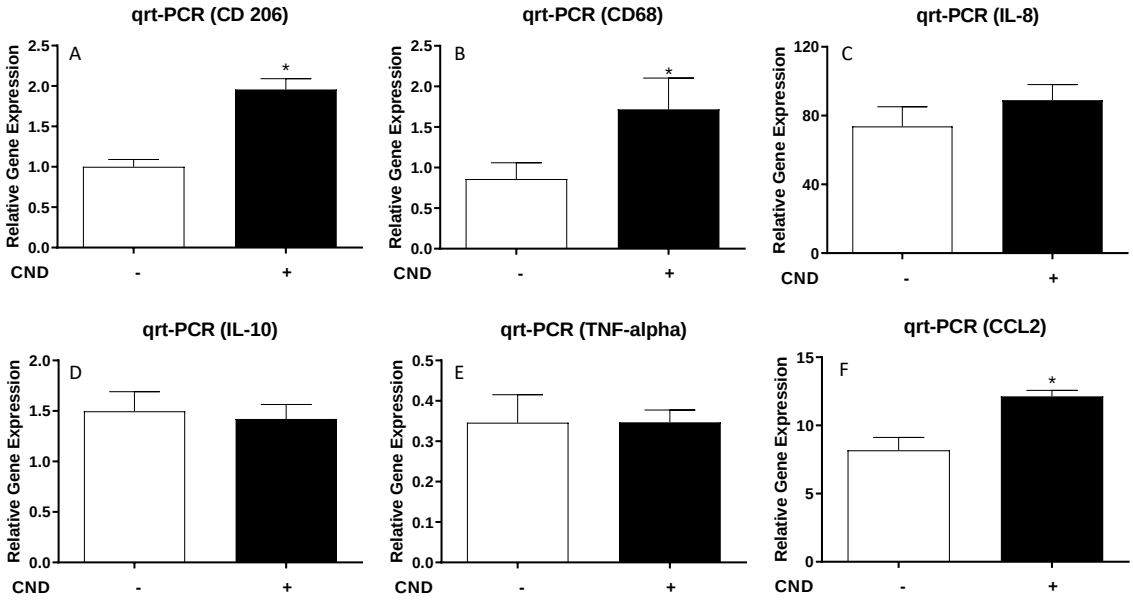

Figure 5. Effect of CNDs on Expression of M1/M2 Biomarkers in Macrophages. THP-1 cells ($1x10_6$) were treated with 3 ng/mL TPA in the presence or absence of 0.1 mg/mL CNDs in RPMI media for 72 hours, upon which media was refreshed. Cells were then left to incubate and mature for another 72 hours. RNA was isolated, converted to cDNA, and probed for CD206, CD68, TNF-alpha, IL-1B, IL-6, IL-8, IL-10, IL-12B, and ARG-1 using SYBR green qRT-PCR reagents via an Applied Biosystems™ StepOne™ Real-Time PCR System. GAPDH was the housekeeping gene. All data represent mean ± SEM. (n = 4-6, *, $P < 0.05$ vs. control).

CND Effect on the Phagocytic Activity of Macrophages

Phagocytic activity is an essential function of macrophages. Macrophages that absorb an excess of ox-LDL turn into foam cells, which are the main component of the necrotic plaque that settles on an artery bed [7]. In order to analyze the effect of CNDs on the phagocytic function of THP-1 monocyte-derived macrophages, THP-1 cells were co-treated with 3 ng/mL TPA and with or without CNDs st 0.1 mg/mL with similar incubation periods as denoted previously. Cells were harvested and incubated in a 96-well plate for 18 hours. Before this incubation period, a sample of control cells was treated with 1000 ng/mL TPA so as to activate macrophages (positive control). Next, cells were treated for 2 hours with a suspension of fluorescent-labeled *Escherichia coli*. Lastly, cells were treated with a Trypan Blue suspension for 1 minute before analysis in a plate reader. Our results indicate that THP-1 monocytes treated with 0.1 mg/mL CNDs during the differentiation process exhibit a significant increase ($P<0.05$) in phagocytic activity (Fig. 6).

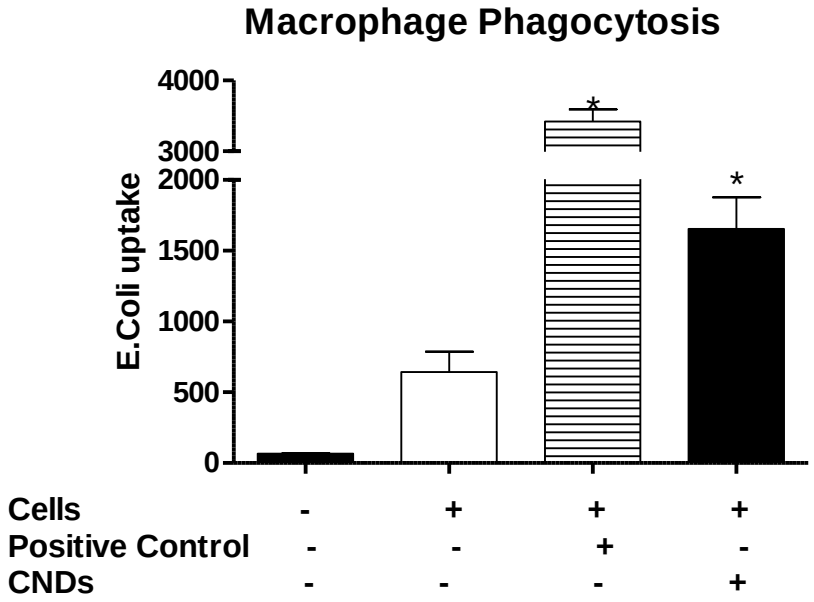

Figure 6. Increase in Phagocytic Activity in CND Co-treated Cells. THP-1 cells ($2x10_6$) were treated with 3 ng/mL TPA in the presence or absence of 0.1 mg/mL CNDs. Cells were incubated for a period of 72 hours, upon which media was refreshed, and followed by another incubation period of 72 hours. Cells were harvested and a sample of control cells were treated with 1000 ng/mL TPA to serve as a positive control. Cells were distributed in a 96-well plate and left to incubate for 18 hours. Treatment of cells with fluorescent *E. coli* suspension followed for 2 hours, upon which the suspension was removed. Cells were finally treated with Trypan Blue. Removal of Trypan Blue preceded the reading in a BioTek™ Synergy 2.0 plate reader. All data represent mean ± SEM. (n = 5, *, $P < 0.05$ vs. control).

Potential Uptake Routes of CNDs into Macrophages

In order to exert intracellular effects, xenobiotics often need to cross the plasma membrane. Nanoparticles are an example of xenobiotics, and recently, uptake routes have become characterized. Hara et al. demonstrated that pre-treatment of THP-1 monocyte-derived macrophages with cytochalasin D, a potent inhibitor of actin polymerization, led to a decrease in the uptake of nano-silica particles [36]. This supports the notion that nanoparticles may mainly enter the cell through phagocytosis.

In order to characterize potential uptake routes of CNDs into macrophages, I differentiated THP-1 monocytes with 3 ng/µL TPA with incubation periods as described previously. Treatment with or without a variety of chemical inhibitors for 30 minutes ensued (with the exception of mercury chloride for 15 minutes) before treating cells with 0.1 mg/mL CNDs. Cells were then harvested, placed in a 96-well plate, and analyzed for fluorescence in a plate reader. Our results indicate significant inhibition ($P<0.05$) of CND uptake with the use of Nocodazole, mercury chloride, and N-phenylanthranilic acid (Fig. 8a, Fig. 8b, Fig. 9a). All other inhibitors used did not show a significant inhibition in CND uptake (Fig. 7 a-k, Fig. 9b).

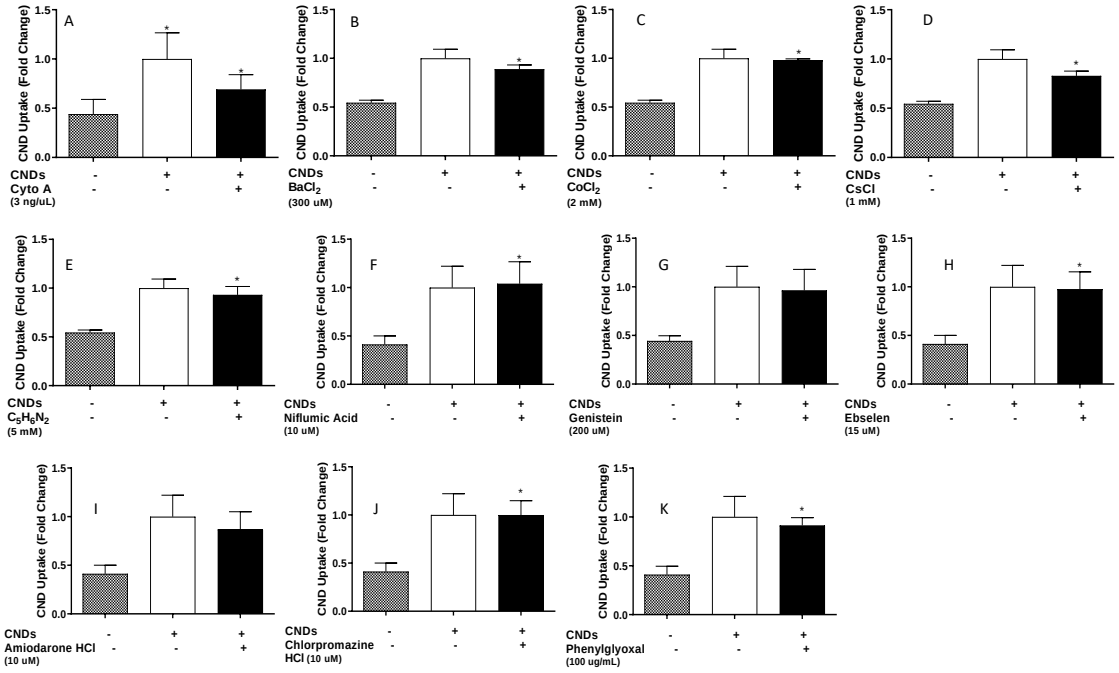

Figure 7. Chemical Inhibitors' Effect on Uptake of CNDs into Macrophages. THP-1 monocyte-derived macrophages ($1x10_6$) were treated for 30 minutes with or without inhibitors (Mercury Chloride for 15 minutes) . Next, cells were treated with 0.1 mg/mL CNDs for 24 hours. Lastly, cells were harvested and placed in a 96-well plate. Fluorescence analysis ensued in a BioTek™ Synergy 2.0 plate reader. All data represent mean ± SEM. (n = 3, *, P<0.005 vs control).

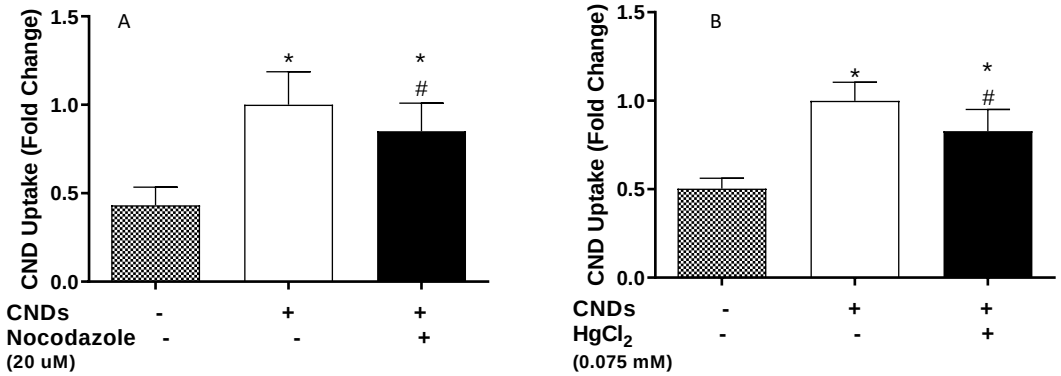

Figure 8. Effect of Nocodazole and $HgCl_2$ on the Uptake of CNDs into Macrophages. THP-1 monocyte-derived macrophages ($1x10_6$) were treated for 30 minutes with or without inhibitors . Next, cells were treated with 0.1 mg/mL CNDs for 24 hours. Lastly, cells were harvested and placed in a 96-well plate. Fluorescence analysis ensued in a BioTek™ Synergy 2.0 plate reader. All data represent mean ± SEM. (n = 4, *, P < 0.05 vs. control, #, P<0.05 vs CND treatment only).

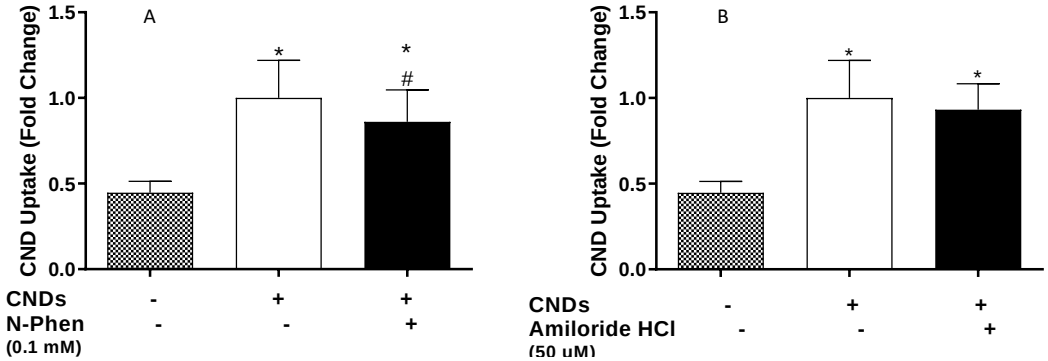

Figure 9. Effect of N-phenylanthranilic Acid and Amiloride Hydrochloride on the Uptake of CNDs into Macrophages. THP-1 monocyte-derived macrophages ($1x10_6$) were treated for 30 minutes with or without inhibitors. Next, cells were treated with 0.1 mg/mL CNDs for 24 hours. Lastly, cells were harvested and placed in a 96-well plate. Fluorescence analysis ensued in a BioTek™ Synergy 2.0 plate reader. All data represent mean ± SEM. (n = 5, *, P < 0.05 vs. CND control, #, P<0.05 vs CND treatment only).

With data indicating inhibition in CND uptake of cells treated with nocodazole, n-phenylanthranilic acid, and mercury chloride, I decided to test the effects of these inhibitors on cell viability. Cells were differentiated as previously described. Treatment with the previously mentioned inhibitor concentrations followed. After refreshing culture media (so as to remove the presence of the inhibitors, cells were left to incubate for 24

hours. Cell viability was tested using previously mentioned Trypan Blue cell count and ViaCount protocols. Our results indicate no significant decrease in the viability of macrophages at any designated concentration of each inhibitor in both the Trypan Blue (Fig. 10) and ViaCount analyses (Fig. 11a). Representative flow cytometric analysis demonstrates no change in the percentage of live cells present in the upper left quadrant for any cells treated with inhibitors (Fig. 11b).

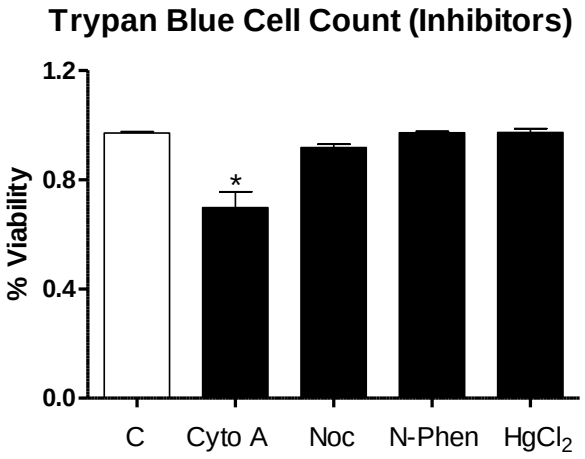

Figure 10. Effect of Chemical Inhibitors on the Viability of Cells (Trypan Blue). THP-1 monocyte-derived macrophages ($1x10_6$) were treated for 30 minutes with either Cytochalasin A (3ug/mL), Nocodazole (20 mM), N-Phenylanthranilic acid (0.1 mM), or Mercury Chloride (0.075 mM) for 15 minutes. With media refreshed. cells were then incubated for a period of 24 hours. A viability analysis was then performed with a hemocytometer cell count using Trypan Blue. All data represent mean ± SEM. (n = 3, *, $P < 0.05$ vs. control).

A

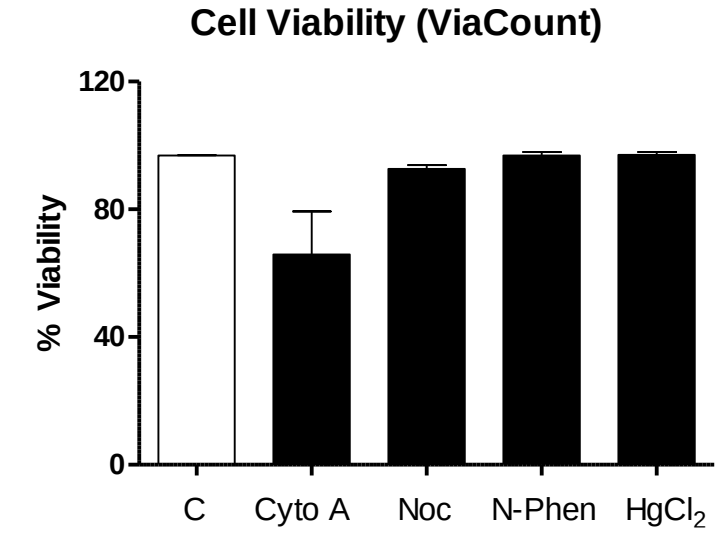

B

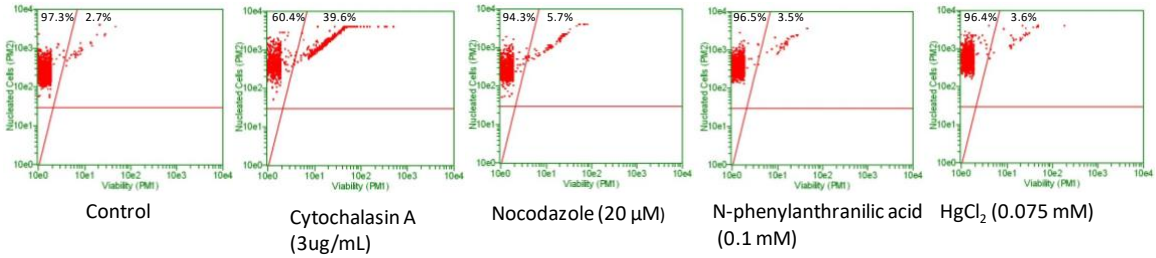

Figure 11. Effect of Chemical Inhibitors on the Viability of Cells (ViaCount). THP-1 monocyte-derived macrophages ($1x10_6$) cultured as mentioned previously, then harvested, resuspended in HBSS, and treated for 30 minutes with either, Nocodazole (20 mM), N-Phenylanthranilic acid (0.1 mM), or Mercury Chloride (0.075 mM) for 15 minutes. Cells were then incubated for a period of 24 hours before treatment with ViaCount reagent. A viability analysis was then performed using a Guava® easyCyte™ Flow Cytometer (Single Sample System). All data represent mean ± SEM. (n = 3).

Potential Cellular Release Routes of CNDs

Currently, no report exists that showcases evidence of CNDs exiting cells. Understanding whether or not this nanoparticle exits cells after uptake is vital information in exploring its potential as a treatment option for atherosclerosis. As such, cells were differentiated as mentioned previously, followed by treatment with 0.1 mg/mL CNDs for 24 hours. The cells were then pelleted, and the supernatant removed after periods of 15, 30, 45, and 60 minutes. The supernatants were placed in a 96-well plate, and analyzed for fluorescence in a plate reader. Our results indicate significant increases ($P<0.05$) in the release of CNDs into the surrounding solution at all time points (Fig. 12).

Considering our data indicated evidence of CND uptake routes while employing chemical inhibitors, I decided to employ those exhibiting significant difference once again. Cells were differentiated in the same manner as in the uptake study. Treatment with 0.1 mg/mL CNDs followed for 24 hours, upon which cells were treated with the previously mentioned concentrations of nocodazole, N-phenylanthranilic acid, and mercury chloride. Next, the cells were pelleted, and the supernatant was removed and placed in a 96-well plate. Lastly, the supernatant was placed in a plate reader for fluorescence quantification.

Our results indicate a significant ($P<0.05$) increase in the release of CNDs from cells treated with 20 μM nocodazole (Fig 13). We did not observe any significant effect on the release of CNDs with N-phenylanthranilic acid or mercury chloride (Fig 13).

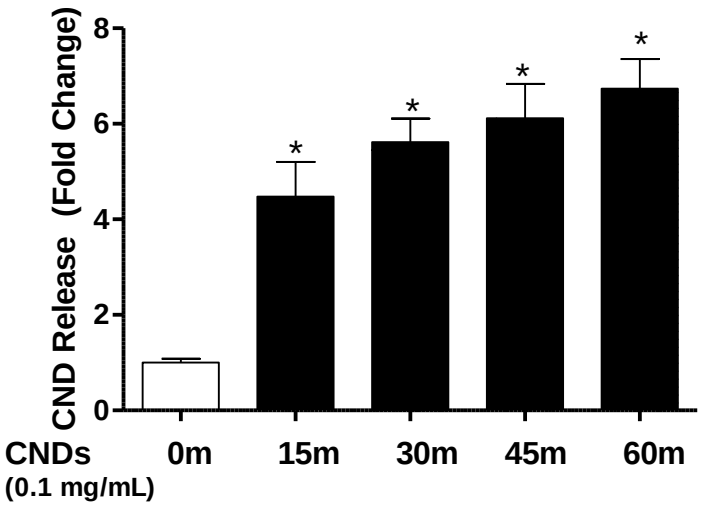

Figure 12. CND Release in Macrophages. THP-1 monocyte-derived macrophages ($3x10_6$) were treated for 24 hours with 0.1 mg/mL CNDs. Next, cells were harvested, pelleted, and media was removed. Pellet was resuspended in HBSS, followed by incubation periods of 15, 30, 45, and 60 minutes. Cells were then pelleted again, and the supernatant removed. Lastly, the supernatant was placed in a 96-well plate. Fluorescence analysis ensued in a BioTek™ Synergy 2.0 plate reader. All data represent mean ± SEM. (n = 3, *, $P < 0.05$ vs. control).

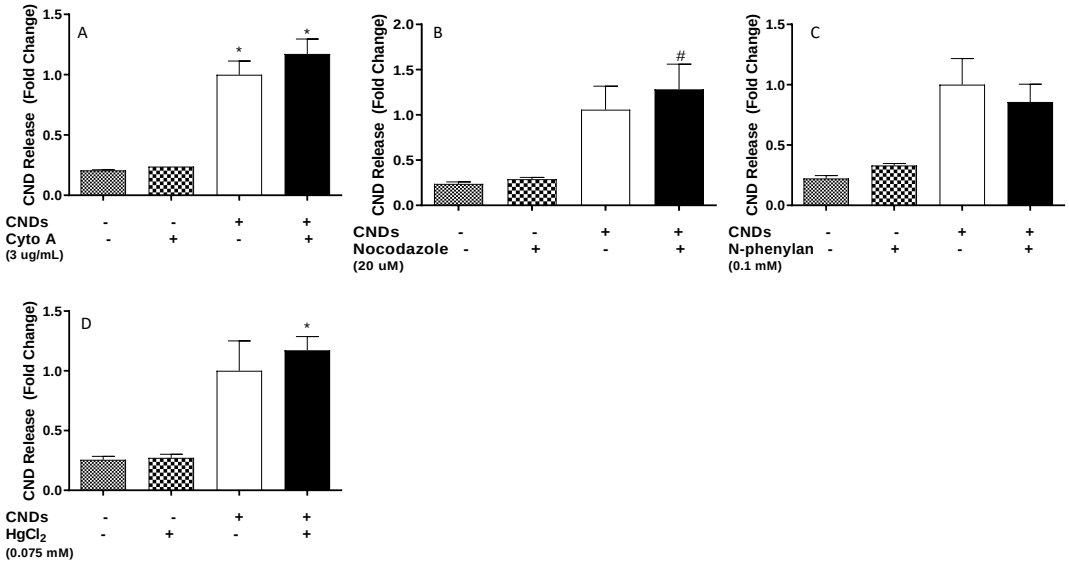

Figure 13. Inhibitor Effect on CND Release in Macrophages. THP-1 monocyte-derived macrophages ($3x10_6$) were treated for 24 hours with 0.1 mg/mL CNDs. Next, cells were harvested, pelleted, and media was removed. Pellet was resuspended in HBSS and treated with or without 20 uM Nocodazole for 30 minutes. Lastly, cells were pelleted and the supernatant placed in a 96-well plate. Fluorescence analysis ensued in a BioTek™ Synergy 2.0 plate reader. All data represent mean ± SEM. (n = 3, *, $P < 0.05$ vs. control, #, $p<0.05$ vs CND treatment only).

CHAPTER IV

DISCUSSION

Macrophages play an important role as mediators of atherosclerosis. For this reason, they are highly sought targets when studying the disease state. CNDs are recently-discovered carbon-based nanomaterials reported to have sizes of 10 nm or less, and also exhibit favorable qualities for use in biomedical application [37]. Collectively, our study represents an initiatory attempt at understanding the interactions of CNDs and macrophages involved in atherosclerosis. Our analysis included studying changes in macrophage biomarker expression. In addition, we studied the effect of CNDs on the phagocytic activity of macrophages. Lastly, we investigated possible uptake and release routes of this nanoparticle.

Macrophages play a crucial intermediary role in the atherosclerosis disease state. The overabundance of settling macrophages and foam cells, due to an excess of lipoprotein ingestion, leads to the emergence of plaque. These macrophages exacerbate the inflammatory microenvironment by secreting pro-inflammatory cytokines to different cell types [6]. A side effect of this process is an excessive dysregulation of macrophage polarization, causing circulating monocytes to differentiate into pro-inflammatory macrophages (M1) in abundance.

As a model, THP-1 human monocyte-derived macrophages were utilized. These monocytes exhibit a homogenous genetic background and differentiate into adherent

macrophages upon exposure to 12-O-tetradecanoylphorbol-13-acetate (TPA). The cell line is resembling of primary monocytes/macrophages, which made it an ideal model for our purposes [38]. These macrophages are characterized by an increase in expression of scavenger receptors while simultaneously reducing LDL receptor expression [39]. Due to their ability to absorb modified lipoproteins and convert to foam cells, THP-1 monocyte-derived macrophages act as a representative model to study macrophage involvement in atherogenesis. In fact, this model has seen extensive use in recent years, appearing in several *in vitro* studies regarding monocyte/macrophage drug transport, signaling, and function [40]. The favorable increase in CD 206 (a macrophage biomarker) expression observed at 3 ng/μL TPA confirmed monocyte differentiation (Fig. 2). With this result, and previously mentioned properties, THP-1 monocyte-derived macrophages became a useful model to analyze the effects of CNDs on the phagocytic activity of macrophages and their expression of biomarkers.

Circulating monocytes that are activated through receptor-ligand binding differentiate into M1 (pro-inflammtory) or M2 (anti-inflammatory) macrophages. This is typically dependent on the immunological response in need. M1 macrophages typically eliminate xenobiotics through phagocytosis and promote the local inflammatory environment. In an atherogenic state, M1 macrophages aim to phagocytose modified lipoproteins in an effort to clear cholesterol. They also extend the inflammatory response by secreting several pro-inflammatory cytokines such as TNF-alpha, IL-1, IL-6, and IL-12 [8]. These cytokines signal additional circulating monocytes to differentiate into M1 macrophages, as well as a host of other cell types involved in immunity. In addition to the

previously mentioned cytokines, M1 macrophages exhibit a variety of biomarkers. *In vitro* studies identify M1 macrophages by the up-regulation of certain receptors such as CD 64, 68, and 80 [13, 41]. Though crucial for host defense, the functions of M1 macrophages can be expropriated during disease states, resulting in dysregulated inflammation [42]. M2 macrophages, in contrast, promote tissue repair, clear cellular debris, and secrete anti-inflammatory cytokines [43]. The presence of M2 macrophages is associated with regressing plaques. Biomarkers of M2 macrophages include anti-inflammatory cytokines such as IL-4, IL-10, and IL-13, as well as a variety of surface receptors that include CD 206, CD CD 23, and CD 163. As a commonality, both types exhibit phagocytic function.

Phagocytic activity is among the most important functions of macrophages. As a form of endocytosis, phagocytosis is defined by the use of a cell membrane to engulf extracellular particles, allowing them entrance into the cell's cytoplasm. As key players of the immune system, macrophages ingest a variety of particles including microbes, modified lipids, and even dead cells entirely [44]. The phagocytic function of macrophages, as well as other roles in immunological responses, makes macrophages a popular target for therapeutic testing. Despite this popularity, no research has been committed to studying the effects of CNDs on the phagocytic activity of primary macrophages. Our study provides a novel insight into this matter. As shown in Figure 6, THP-1 monocyte-derived macrophages that were treated with 0.1 mg/mL CNDs during the differentiation process exhibit an increase in phagocytic activity.

The expressions of macrophage biomarkers, from treatment with CNDs during the differentiation process of THP-1 monocyte-derived macrophages, were analyzed to further understand if this boost in phagocytic function favors M1 or M2 polarization. Cells treated with 0.1 mg/mL CNDs demonstrated a significant increase in CCL-2 and CD 68, which are both considered M1 biomarkers (Fig. 5b, 5f). Several studies have demonstrated that M1 macrophages accumulate cholesterol via modified, atherogenic LDL (e.g. ox-LDL) as opposed to native LDL [6]. Modified LDL is internalized through phagocytosis. In the case of atherosclerosis, M1 macrophages recognize ox-LDL by means of scavenger receptors including scavenger receptor A, CD 36, and CXCL16 [6, 45]. CD 68 and its mouse ortholog macrosialin have also been recognized as receptors for ox-LDL [46]. The excessive uptake of cholesterol from modified lipoproteins leads to a dysregulation of lipid metabolism within M1 macrophages. This dysregulation results in a build-up of free cholesterol, which is toxic unlike other forms such as cholesteryl ester [45]. Among the effects of free cholesterol is the activation of stress responses in the endoplasmic reticulum, which prevents the re-esterification of cholesterol. Normally, macrophages submit cholesterol through a process of esterification that permits a series of transporters to expel them from the cell [6]. ER stress thus promotes the build-up of free cholesterol in macrophages, which in turn furthers the creation of foam cells. This knowledge, combined with the increase in both M1 biomarkers observed, would seem to suggest CNDs tilt the polarization of macrophages towards M1.

However, our results also demonstrated a significant increase in the expression of CD 206, a prominent M2 biomarker (Fig. 5a). This receptor has functionality in the

phagocytosis of different bacteria [15]. The increase observed in expression of this receptor may very well explain the increase observed in phagocytic activity, considering CD 206 recognizes *E. coli* [47]. Additionally, CD 206 serves as a regulator of adipocyte progenitors [48]. This result seemingly counters the increase in M1 biomarkers mentioned previously, and suggests polarization towards M2 phenotypes.

The differentiation and polarization of macrophages towards M1 or M2 phenotypes is governed by several factors. Toll-like receptors (TLRs) play a crucial role in the differentiation of M1 macrophages. Modified lipoproteins and pro-inflammatory cytokines can act on TLRs and activate the Nf-κB pathway, a key inducer of pro-inflammatory gene transcription [9]. Lipopolysaccharides (LPS), as found on the outer membrane of Gram-negative bacteria, also stimulate TLRs to activate the Nf-κB pathway. Anti-inflammatory cytokines such as, IL-4 and IL-10, bind to their respective receptors on the cell membrane and stimulate Janus-kinase signal transducers (JAK). JAK transducers activate isoforms of STAT, which in turn repress inducers of pro-inflammatory cytokines and activate production of anti-inflammatory cytokines [42]. STAT3, for instance, is connected to repression of the Nf-κB pathway. Despite the numerous signaling pathways involved in macrophage differentiation, ROS is considered a trademark inducer in this process, necessary for both M1 and M2 differentiation [49, 50].

Although the exact mechanisms through which CNDs act on the polarization of macrophages are quite unexplored, mounting evidence presupposes the involvement of reactive oxygen species (ROS) as a key player. First, THP-1 monocytes have been

confirmed to produce ROS upon differentiation with TPA [49]. Secondly, a recent study has demonstrated that scavenging ROS species inhibits polarization of macrophages to an M2 phenotype when treated with redox-active drug MnTE-2-PyP^{5+}, partly through suppression of STAT3 [50]. This evidence indicates that ROS plays a role in the activation of STAT3. Thirdly, mounting evidence demonstrates the capability of CNDs as antioxidants and scavengers of ROS. Nitrogen and sulfur co-doped CNDs are able to scavenge DPPH+ radicals [32]. CNDs have also shown capability of scavenging superoxide and hydroxyl radicals [33]. Because of this, we can infer that CNDs may block the activation of STAT3, and therefore inhibit the repression of proinflammatory gene transcription. This indicates that our observed increase in CCL2 is consistent with the previously mentioned report. However, the increase in CD 206, denoting M2 polarization, also suggests that CNDs may not elicit its effects in a similar manner to redox-active compounds like MnTE-2-Pyp^{5+}. Perhaps CNDs tip the polarization of macrophages to an M1 state, while also targeting expression of receptors tied to phagocytosis, regardless of their functionality in pro or anti-inflammation.

Our study of the effect of CNDs on the phagocytic activity and expression of biomarkers in macrophages possess certain limitations that must be addressed in future studies. CNDs were treated during the differentiation process of THP-1 monocytes. Treating CNDs pre and post differentiation may showcase entirely different results. At the same time, the biomarkers analyzed are of a limited number. Expression changes in CD 206, CD 68, and CCL2 suggest interesting ideas, but our results also showcased no discernable effect in the expression of IL-8, IL-10, and TNF-α cytokines (Fig. 5c-e).

Additionally, there are a myriad of M1 and M2 cytokines and surface receptors that must be analyzed before any definite conclusions can be made. Our phagocytosis assay also employed fluorescently-labeled *E.*coli as a pathogen for macrophages to absorb. Modified lipids should be used instead of bacterial pathogens in order to designate CNDs as an effective or ineffective treatment option against atherosclerosis. Last but not least, we did not establish a dose-dependent effect of CNDs on both phagocytic activity and expression of M1/M2 biomarkers.The Treatment of CNDs in this study was limited to 0.1 mg/mL. Higher and lower concentrations of CNDs must be utilized in further research projects.

To further deepen our understanding of the interaction of CNDs and macrophages the final aims of this study examined potential uptake and release routes of CNDs into THP-1 monocyte-derived macrophages. Previous studies have denoted the involvement of actin, microtubules, and endocytic pathways in the uptake of nanoparticles: (i) Dos Santos et al. showed that use of chlorpromazine, genistein, nocodazole, and Cytochalasin A inhibited the uptake of carboxylated polystyrene nanoparticles via clathrin-mediated endocytosis in various cell lines [51]. Chlorpromazine suppresses clathrin disassembly and receptor recycling in the cell membrane. Genistein specifically inhibits tyrosine kinase receptors involved in calveolae-mediated endocytosis. Nocodazole and Cytochalasin-A disrupt microtubule and actin filaments. (ii) Park et al. demonstrated that amiloride successfully inhibited the uptake of hydrophobically modified glycol chitosan nanoparticles (HGC-NPs). Amiloride inhibits macropinocytosis by suppressing Na^+/H^+ exchange [52]. These studies suggest that nanoparticles may enter cells primarily through

endocytic pathways. Nonetheless, no research has been committed in utilizing these inhibitors to characterize potential uptake routes of CNDs into macrophages.

In addition to the previously mentioned inhibitors, our study employed a variety of chemical inhibitors designed to cover multiple cellular entrance routes. Among the list were mercury chloride ($HgCl_2$), known to inhibit aquaporin channels [53]. Barium chloride and 4-aminopyridine also served to block potassium channels [54]. The extensive list of inhibitors also included niflumic acid, ebselen, and phenylglyoxal. Uptake analysis demonstrated significant inhibition in the uptake of CNDs when macrophages were treated with nocodazole, N-phenylanthranilic acid, and mercury chloride ($HgCl_2$) (Fig. 8, Fig. 9). Changes were also observed with other inhibitors, however, no significant trend could be established (Fig. 7). Treatment with cytochalasin A demonstrated inhibition of CND uptake. However, upon performing cell viability tests, it was discovered that Cytochalasin A had adverse effects on macrophages (Fig. 10, Fig. 11). This likely represents the observed inhibition of CND uptake as a causation of cell death, which would reduce the fluorescent signal of CNDs, giving the appearance of uptake inhibition.

The observed inhibition of CND uptake as a result of treatment with nocodazole suggests that CNDs can gain entrance into cells through endocytic pathways. N-phenylanthranilic acid acts as a chloride channel blocker in cell membranes. The CNDs utilized in this study exhibit negatively-charged surface functional groups. Given that chloride is a negatively charged molecule, the passage of CNDs through this channel has merit. This result also gives rise to an interesting notion. Though small even in the

nanoparticle scale (~10 nm), CNDs are still relatively large in comparison to chloride ions (~0.2 nm). Our results suggest that depending on the surface groups tailored to CNDs, size may not be an issue in gaining entrance into cells through ion channels. Nanoparticles have demonstrated capability of binding to carrier proteins in order to enter plant cells through aquaporins, ion channels, or endocytosis [55]. These findings explain the inhibition of uptake observed with treatment of macrophages with $HgCl_2$, and suggest CNDs may pass through aquaporins in similar fashion.

The efficacy of the interaction of nanoparticles and their target cell is judged not just by their ability to enter a cell, but also by the time it takes to be metabolized or released. Chithrani et al. demonstrated imaging of gold nanoparticles exiting cells in packaged vesicles [56]. These findings provide evidence for nanoparticle release through exocytosis. Prior to this study, however, it was unknown whether or not CNDs are released from cells or metabolized into different molecules. Our results provide evidence for the release of CNDs from macrophages in a time-dependent fashion (Fig. 12). In an attempt to elucidate release routes, treatment of cells with inhibitors that demonstrated effect on the uptake of CNDs followed. Nocodazole was the sole chemical that elicited a change in the release quantity of CNDs (Fig. 13).

Microtubules represent a type of cytoskeletal structure that functions to transport materials throughout a cell's cytoplasm. These structures act as tracks for motor proteins dynein and kinesin as they deliver cargo to different parts of the cell [57]. Motor proteins deliver many materials to the cell's membrane for exocytosis as well. Because nocodazole is a microtubule disruptor, it is logical to assume inhibition of exocytosis of

CNDs. Our results show the opposite; CND release was increased with treatment of nocodazole (Fig. 13). These results indicate that CNDs likely exit cells through other routes apart from exocytosis. Blocking exocytosis as an efflux route may boost exit through other available channels or pathways. Our study on release was very limited, considering only inhibitors that showed effect during uptake analysis were used. Future studies on the release of CNDs will employ all previously mentioned inhibitors.

In summary, our results provide novel evidence of the interaction of CNDs and macrophages involved in atherosclerosis. CNDs were confirmed to be nontoxic at different concentrations by performing Trypan Blue cell counts and ViaCount flow cytometry. Our PCR results indicate a significant increase in the expression of at least one M2 biomarker (CD 206), and increases in M1 biomarkers CCL2 and CD 68. Two of these biomarkers are involved in the phagocytic function of macrophages. Though no fixed conclusions can yet be assumed regarding how CNDs affect macrophage polarization, our phagocytosis assay results indicate that CND treatment during the differentiation process boosts phagocytic activity, possibly due to the scavenging of ROS. Lastly, we also determined potential cellular uptake and release routes of CNDs. Results showcased inhibitions of CND uptake in cells treated with nocodazole, n-phenylanthranilic acid, and mercury chloride, providing evidence for entrance routes in the form of endocytosis, chloride and water channels. Treatment of cells with nocodazole also boosted CND release, suggesting the idea that inhibiting exocytosis may shun CND release through other routes. Collectively, these results yield a deeper understanding in the interaction between macrophages involved in atherosclerosis and CNDs.

REFERENCES

1. Joseph, P., et al., *Reducing the Global Burden of Cardiovascular Disease, Part 1: The Epidemiology and Risk Factors.* Circ Res, 2017. **121**(6): p. 677-694.
2. Li, H., S. Horke, and U. Forstermann, *Vascular oxidative stress, nitric oxide and atherosclerosis.* Atherosclerosis, 2014. **237**(1): p. 208-19.
3. Soeki, T. and M. Sata, *Inflammatory Biomarkers and Atherosclerosis.* Int Heart J, 2016. **57**(2): p. 134-9.
4. Hoefer, I.E., et al., *Novel methodologies for biomarker discovery in atherosclerosis.* Eur Heart J, 2015. **36**(39): p. 2635-42.
5. Pamukcu, B., G.Y. Lip, and E. Shantsila, *The nuclear factor--kappa B pathway in atherosclerosis: a potential therapeutic target for atherothrombotic vascular disease.* Thromb Res, 2011. **128**(2): p. 117-23.
6. Bobryshev, Y.V., et al., *Macrophages and Their Role in Atherosclerosis: Pathophysiology and Transcriptome Analysis.* Biomed Res Int, 2016. **2016**: p. 9582430.
7. Yu, X.H., et al., *Foam cells in atherosclerosis.* Clin Chim Acta, 2013. **424**: p. 245-52.
8. Chistiakov, D.A., et al., *The impact of interferon-regulatory factors to macrophage differentiation and polarization into M1 and M2.* Immunobiology, 2018. **223**(1): p. 101-111.
9. Ruytinx, P., et al., *Chemokine-Induced Macrophage Polarization in Inflammatory Conditions.* Front Immunol, 2018. **9**: p. 1930.
10. Brocheriou, I., et al., *Antagonistic regulation of macrophage phenotype by M-CSF and GM-CSF: implication in atherosclerosis.* Atherosclerosis, 2011. **214**(2): p. 316-24.
11. Chistiakov, D.A., et al., *Macrophage phenotypic plasticity in atherosclerosis: The associated features and the peculiarities of the expression of inflammatory genes.* Int J Cardiol, 2015. **184**: p. 436-45.
12. Moore, K.J., F.J. Sheedy, and E.A. Fisher, *Macrophages in atherosclerosis: a dynamic balance.* Nat Rev Immunol, 2013. **13**(10): p. 709-21.
13. Tarique, A.A., et al., *Phenotypic, functional, and plasticity features of classical and alternatively activated human macrophages.* Am J Respir Cell Mol Biol, 2015. **53**(5): p. 676-88.
14. Rojas, J., et al., *Macrophage Heterogeneity and Plasticity: Impact of Macrophage Biomarkers on Atherosclerosis.* Scientifica (Cairo), 2015. **2015**: p. 851252.
15. Shrivastava, R. and N. Shukla, *Attributes of alternatively activated (M2) macrophages.* Life Sci, 2019. **224**: p. 222-231.
16. Corrado, E., A. Mignano, and G. Coppola, *Use of statins in patients with peripheral artery disease.* Trends Cardiovasc Med, 2019.
17. Bouitbir, J., et al., *Mechanisms of statin-associated skeletal muscle-associated symptoms.* Pharmacol Res, 2019: p. 104201.
18. Park, J.G. and G.T. Oh, *Current pharmacotherapies for atherosclerotic cardiovascular diseases.* Arch Pharm Res, 2019. **42**(3): p. 206-223.

19. Fassaert, L.M. and G.J. de Borst, *Technical improvements in carotid revascularization based on the mechanism of procedural stroke.* J Cardiovasc Surg (Torino), 2019. **60**(3): p. 313-324.
20. Rezaei, R., et al., *The Role of Nanomaterials in the Treatment of Diseases and Their Effects on the Immune System.* Open Access Maced J Med Sci, 2019. **7**(11): p. 1884-1890.
21. Ovais, M., M. Guo, and C. Chen, *Tailoring Nanomaterials for Targeting Tumor-Associated Macrophages.* Adv Mater, 2019. **31**(19): p. e1808303.
22. Weissleder, R., M. Nahrendorf, and M.J. Pittet, *Imaging macrophages with nanoparticles.* Nat Mater, 2014. **13**(2): p. 125-38.
23. Cho, W.S., et al., *Progressive severe lung injury by zinc oxide nanoparticles; the role of Zn2+ dissolution inside lysosomes.* Part Fibre Toxicol, 2011. **8**: p. 27.
24. Wang, X., et al., *Dispersal state of multiwalled carbon nanotubes elicits profibrogenic cellular responses that correlate with fibrogenesis biomarkers and fibrosis in the murine lung.* ACS Nano, 2011. **5**(12): p. 9772-87.
25. Ding, C., A. Zhu, and Y. Tian, *Functional surface engineering of C-dots for fluorescent biosensing and in vivo bioimaging.* Acc Chem Res, 2014. **47**(1): p. 20-30.
26. Roy, P., et al., *Photoluminescent carbon nanodots: synthesis, physicochemical properties and analytical applications.* Materials Today, 2015. **18**(8): p. 447-458.
27. Miao, P., et al., *Recent advances in carbon nanodots: synthesis, properties and biomedical applications.* Nanoscale, 2015. **7**(5): p. 1586-95.
28. Das, R., et al., *Can We Optimize Arc Discharge and Laser Ablation for Well-Controlled Carbon Nanotube Synthesis?* Nanoscale Res Lett, 2016. **11**(1): p. 510.
29. Liu, H., T. Ye, and C. Mao, *Fluorescent carbon nanoparticles derived from candle soot.* Angew Chem Int Ed Engl, 2007. **46**(34): p. 6473-5.
30. Liang, Y., et al., *Simple hydrothermal preparation of carbon nanodots and their application in colorimetric and fluorimetric detection of mercury ions.* Analytical Methods, 2015. **7**(18): p. 7540-7547.
31. Zhang, W., Z. Zeng, and J. Wei, *Electrochemical Study of DPPH Radical Scavenging for Evaluating the Antioxidant Capacity of Carbon Nanodots.* The Journal of Physical Chemistry C, 2017. **121**(34): p. 18635-18642.
32. Zhang, W., et al., *Antioxidant Capacity of Nitrogen and Sulfur Codoped Carbon Nanodots.* ACS Applied Nano Materials, 2018. **1**(6): p. 2699-2708.
33. Das, B., et al., *Carbon nanodots from date molasses: new nanolights for the in vitro scavenging of reactive oxygen species.* Journal of Materials Chemistry B, 2014. **2**(39): p. 6839-6847.
34. Riss, T., et al., *Cytotoxicity Assays: In Vitro Methods to Measure Dead Cells*, in *Assay Guidance Manual*, G.S. Sittampalam, et al., Editors. 2004: Bethesda (MD).
35. Cooper, A.M. and S.A. Khader, *IL-12p40: an inherently agonistic cytokine.* Trends Immunol, 2007. **28**(1): p. 33-8.
36. Hara, K., et al., *Interferon-tau attenuates uptake of nanoparticles and secretion of interleukin-1beta in macrophages.* PLoS One, 2014. **9**(12): p. e113974.
37. Anwar, S., et al., *Recent Advances in Synthesis, Optical Properties, and Biomedical Applications of Carbon Dots.* ACS Applied Bio Materials, 2019. **2**(6): p. 2317-2338.

38. Chanput, W., V. Peters, and H. Wichers, *THP-1 and U937 Cells*, in *The Impact of Food Bioactives on Health: in vitro and ex vivo models*, K. Verhoeckx, et al., Editors. 2015: Cham (CH). p. 147-159.
39. Qin, Z., *The use of THP-1 cells as a model for mimicking the function and regulation of monocytes and macrophages in the vasculature.* Atherosclerosis, 2012. **221**(1): p. 2-11.
40. Chanput, W., J.J. Mes, and H.J. Wichers, *THP-1 cell line: an in vitro cell model for immune modulation approach.* Int Immunopharmacol, 2014. **23**(1): p. 37-45.
41. Ren, S., et al., *Expression of NF-kappaB, CD68 and CD105 in carotid atherosclerotic plaque.* J Thorac Dis, 2013. **5**(6): p. 771-6.
42. Tugal, D., X. Liao, and M.K. Jain, *Transcriptional control of macrophage polarization.* Arterioscler Thromb Vasc Biol, 2013. **33**(6): p. 1135-44.
43. Ying, B., et al., *M2 Macrophages as a Potential Target for Antiatherosclerosis Treatment.* Neural Plasticity, 2019.
44. Gordon, S. and A. Pluddemann, *Tissue macrophages: heterogeneity and functions.* BMC Biol, 2017. **15**(1): p. 53.
45. Moore, K.J., et al., *Macrophage Trafficking, Inflammatory Resolution, and Genomics in Atherosclerosis: JACC Macrophage in CVD Series (Part 2).* J Am Coll Cardiol, 2018. **72**(18): p. 2181-2197.
46. Chistiakov, D.A., et al., *CD68/macrosialin: not just a histochemical marker.* Lab Invest, 2017. **97**(1): p. 4-13.
47. Schulz, D., et al., *In-Depth Characterization of Monocyte-Derived Macrophages using a Mass Cytometry-Based Phagocytosis Assay.* Sci Rep, 2019. **9**(1): p. 1925.
48. Nawaz, A., et al., *CD206(+) M2-like macrophages regulate systemic glucose metabolism by inhibiting proliferation of adipocyte progenitors.* Nat Commun, 2017. **8**(1): p. 286.
49. Tan, H.Y., et al., *The Reactive Oxygen Species in Macrophage Polarization: Reflecting Its Dual Role in Progression and Treatment of Human Diseases.* Oxid Med Cell Longev, 2016. **2016**: p. 2795090.
50. Griess, B., et al., *Scavenging reactive oxygen species selectively inhibits M2 macrophage polarization and their pro-tumorigenic function in part, via Stat3 suppression.* Free Radic Biol Med, 2020. **147**: p. 48-60.
51. dos Santos, T., et al., *Effects of transport inhibitors on the cellular uptake of carboxylated polystyrene nanoparticles in different cell lines.* PLoS One, 2011. **6**(9): p. e24438.
52. Park, S., et al., *Cellular uptake pathway and drug release characteristics of drug-encapsulated glycol chitosan nanoparticles in live cells.* Microsc Res Tech, 2010. **73**(9): p. 857-65.
53. Ismail, M., et al., *Inhibition of the aquaporin 3 water channel increases the sensitivity of prostate cancer cells to cryotherapy.* Br J Cancer, 2009. **100**(12): p. 1889-95.
54. Romero, F., et al., *Aristoteline, an Indole-Alkaloid, Induces Relaxation by Activating Potassium Channels and Blocking Calcium Channels in Isolated Rat Aorta.* Molecules, 2019. **24**(15).
55. Rico, C.M., et al., *Interaction of nanoparticles with edible plants and their possible implications in the food chain.* J Agric Food Chem, 2011. **59**(8): p. 3485-98.
56. Chithrani, B.D. and W.C. Chan, *Elucidating the mechanism of cellular uptake and removal of protein-coated gold nanoparticles of different sizes and shapes.* Nano Lett, 2007. **7**(6): p. 1542-50.

57. Franker, M.A. and C.C. Hoogenraad, *Microtubule-based transport - basic mechanisms, traffic rules and role in neurological pathogenesis.* J Cell Sci, 2013. **126**(Pt 11): p. 2319-29.